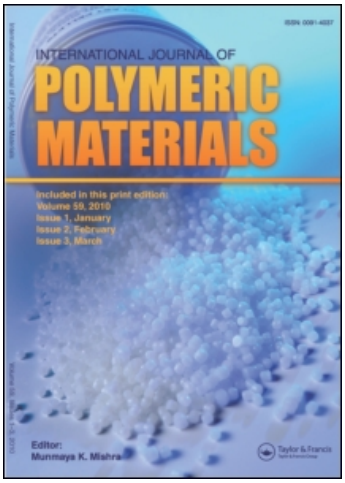

International Journal of Polymeric Materials
Publication details, including instructions for authors and subscription information:
http://www.informaworld.com/smpp/title~content=t713647664

Structure of Nylon-6 from Analysis of Viscoelastic Properties

D. Prevorsek[a]; R. H. Butler[a]
[a] Allied Chemical Corporation Corporate Chemical Research Laboratory, Morristown, N.J

To cite this Article Prevorsek, D. and Butler, R. H.(1972) 'Structure of Nylon-6 from Analysis of Viscoelastic Properties', International Journal of Polymeric Materials, 1: 3, 251 — 277
To link to this Article: DOI: 10.1080/00914037208075288
URL: http://dx.doi.org/10.1080/00914037208075288

Intern. J. Polymeric Mater., 1972, Vol. 1, pp. 251–277

Printed in Great Britain

Structure of Nylon-6 from Analysis of Viscoelastic Properties

D. PREVORSEK and R. H. BUTLER

Allied Chemical Corporation Corporate Chemical Research Laboratory, Morristown, N.J

(*Received March* 21, 1972)

A method is outlined to study the structure property relationship in semicrystalline fibers involving (a) the characterization of structure in terms of the two phase amorphous-crystalline model (size, concentration and orientation of the crystallites, etc.), (b) the analysis of viscoelastic responses in terms of Takayanagi models, and (c) the analysis of diffusion assuming that crystals are essentially impermeable to large dye molecules. The method, which does not require an accurate estimate of the properties of a "completely" amorphous polymer, is applied to a series of oriented nylon 6 fibers. The study, which confirms the validity of the derived equation to describe the diffusion process in semi-crystalline polymers above the glass transition temperature, leads to a quantitative representation of the "efficiency" of crystal reinforcement as a function of the degree of crystallinity.

INTRODUCTION

Mechanical, thermal, radiation, chemical and other treatments can lead to enormous variations in the structure of semicrystalline polymers. Changes in morphology resulting from various treatments involving heat, pressure, plastic deformation, etc. have been studied extensively and much is known about the nature of structural reorganization taking place in polymers under various conditions.

The effect of structural parameters on the mechanical responses, on the other hand, still remains poorly understood despite an ample background in morphology and awareness of the important effects that the morphology of polymers has on mechanical performance. The slow progress in this area of prime practical and theoretical importance can be attributed to several factors. First, in development of a theory of physical properties of semi-

crystalline polymers, one is faced with the fundamental difficulties encountered in treating heterogeneous systems. The morphology of semicrystalline polymers is often so complex that it defies an adequate description or representation by suitable models. Furthermore, the results of morphological studies often appear in a descriptive form which is difficult to express quantitatively in terms of parameters appearing in expressions describing the mechanical behavior of heterogeneous systems.

Some polymeric systems have a structure which is heterogeneous on more than one level (e.g. spherulites, lamellae, extended chain crystals, cilia, etc.). For such systems, a quantitative theory of mechanical properties in terms of structural parameters would involve difficulties of a prohibitive magnitude. In many cases, however, the structure of semicrystalline polymers can be reasonably well represented by a two phase model consisting of crystalline domains dispersed in the amorphous phase or vice versa. These are the systems with which this study is concerned. The mechanical properties of such polymers can be interpreted in terms of the properties of the crystalline and amorphous domains provided we know the volume fraction of crystallites, their average dimensions, their orientation and dispersion characteristics and the nature of the phase boundary. The average dimensions, concentration and orientation of crystallites are estimated from x-ray diffraction data and electron microscopy studies. On the other hand, the characterization of the interphase and its strength, which in morphological studies frequently involves the study of crystallite surfaces with regard to chain folding and the concentration of the tie molecules between the crystallites and the amorphous phase, invariably involves difficult experimental procedures which often lead to ambiguous results.

This study was prompted to a large degree by the desirability of finding a suitable technique to characterize the nature of the interface and the role of the crystallites in the mechanical properties of semicrystalline polymers.

Realizing that the structure of the boundary between the crystallites and the amorphous phase (i.e. the degree of chain folding, or the concentration of tie molecules) should have a considerable effect on the transfer of stress and strain from one phase to another, we speculated that the study of mechanical coupling between phases in combination with a sophisticated morphological analysis could provide valuable information regarding the structure of the crystal-amorphous boundary.

The proposed method involves: a) the characterization of structure in terms of the two phase amorphous-crystalline model (site, concentration, and orientation of the crystallites, etc.) b) the analysis of mechanical coupling between phases in terms of Takayanagi[1] models, and c) the interpretation of mechanical properties assuming a two phase compound system. In principle, such a study should provide information regarding the "efficiency" of

crystallite reinforcement in amorphous matrix structures, the contribution of the amorphous phase to the impact resistance in structure having a crystalline matrix and other responses which are affected by the structures of the interface.

In applying the proposed method, we found that the analysis of mechanical coupling in terms of Takayanagi models is much more complicated than reported in the literature. In particular, we found that in order to apply the method quantitatively, one requires basic polymer characterization data of extreme, and presently unobtainable, accuracy. Thus, in this paper we are primarily concerned with the theory and development of methods for determining the correct coupling models given the present state of polymer characterization methods.

The experimental data are included mostly for purposes of illustration of these methods. An extensive study of the structure of various polymers by the method outlined above, will be presented in subsequent publications.

THEORY

Dynamic mechanical properties (E', E'', tan δ, etc.) measured in isochronal experiments depend on morphological characteristics (degree of crystallinity, orientation, crystallite size, etc.). In particular, the intensities of transitions observed in experiments conducted as a function of temperature are also effected by morphology. Takayanagi has shown that in cases where the properties of the crystalline and amorphous domains are known, the viscoelastic characteristics of semi-crystalline polymers can be reproduced by means of unit cube models shown in Figure 1. There, C is the crystalline and A the amorphous domain with the respective complex moduli E^*_c and E^*_a. With the models A, B, and C the degree of crystallinity equals $(1-\lambda\phi)$ where ϕ and λ are the indicated dimensions of the amorphous domains. With the models D, E, and F, on the other hand, the degree of crystallinity equals $\phi'\lambda'$.

The physical significance of these models can best be illustrated when these systems are considered under applied stress indicated by the arrows. In the model A which is often referred to as a parallel model, both phases are under equal strain. Consequently, in cases where $|E^*_c| \gg |E^*_a|$ the strain in the crystalline phase is negligible. Models B, C, E, and F represent a combination of the parallel-series and series-parallel arrangement. From the morphological point of view, it is important to distinguish between models B and C, which represent systems having a crystalline matrix with the amorphous phase dispersed therein, and models E and F where the situation is reversed. In order to achieve the objectives outlined in the introduction, it is necessary to determine, as accurately as possible, which of these models best describes the

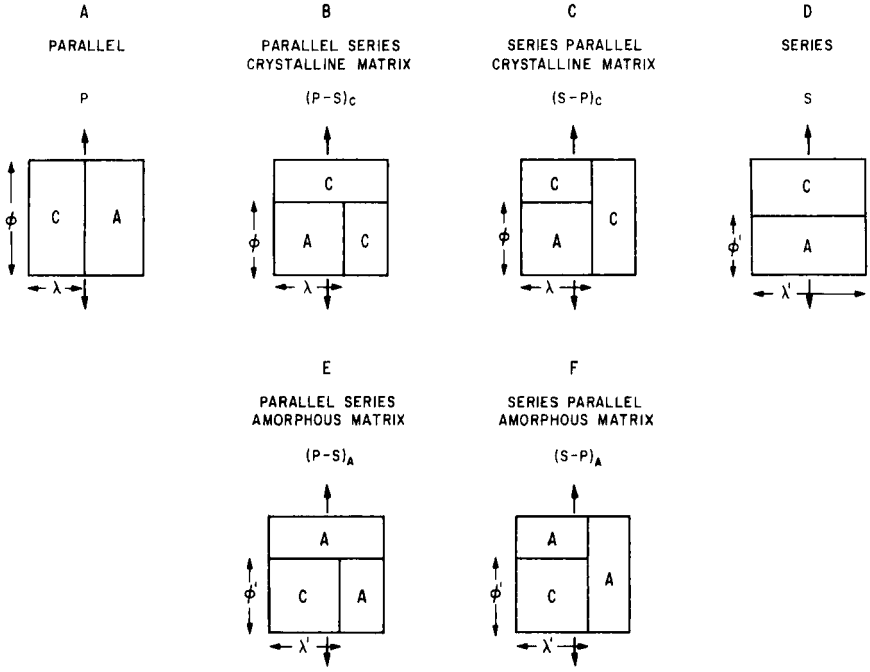

FIGURE 1 Takayanagi mechanical coupling models.

measured mechanical responses. Since the parallel and series models A and D are special cases of the other more general models, the problem will be to select among models B, C, E, and F and determine with least error ϕ and λ (or ϕ' and λ'). The values of crystallinity expressed as $(1-\phi\lambda)$, $(\phi'\lambda')$ or X, will be those determined by standard x-ray diffraction techniques. In order to illustrate the method of selection, it is desirable to examine the functional relationship between the dynamic-mechanical properties of the system: E_s', E_s'', and tan δ_s (of which only 2 are independent since tan δ_s equals E_s''/E_s') and the degree of crystallinity for various modes of load transfer.

Effects of Degree of Crystallinity on E_s', E_s'', and tan δ_s

The expressions for the real part of the complex modulus (E_s) for the various models are shown below:

parallel (Model A):

$$\frac{E_s'}{E_c} = X + \frac{(1-X)}{K} \tag{1}$$

parallel-series crystal matrix (Model B):

$$\frac{E_s'}{E_c} = 1 - \frac{(1 - X)}{\frac{1}{K - 1} + \sqrt{\frac{1 - X}{\sigma}}} \tag{2}$$

series-parallel crystal matrix (Model C):

$$\frac{E_s'}{E_c} = \frac{\frac{K}{K-1} - \sqrt{(1 - X)\,\sigma}}{\frac{K}{K-1} - \sqrt{(1 - X)\,\sigma} + (1 - X)} \tag{3}$$

series (Model D):

$$\frac{E_s'}{E_c} = \frac{1}{(1 - X)K + X} \tag{4}$$

parallel-series amorphous matrix (Model E):

$$\frac{E_s'}{E_c} = \frac{1}{K}\left(1 + \frac{X}{\frac{K}{K-1} - \sqrt{\frac{x}{\sigma}}}\right) \tag{5}$$

series-parallel amorphous matrix (Model F):

$$\frac{E_s'}{E_c} = \frac{1}{K}\left(\frac{1}{1 - \frac{X}{\frac{K}{K-1} + \sqrt{X\sigma}}}\right) \tag{6}$$

$$K \equiv \frac{E_c}{E_A'},$$

From the above expressions it is apparent that E_s' for models B, C, E, and F depends on both the degree of crystallinity X and the ratio of λ to ϕ (or λ' to ϕ') which we have defined as σ (or σ'). In order to illustrate the essential features of the variation of E_s with crystallinity which these expressions exhibit, we present the corresponding plots in Figure 2 for $\sigma = 1$. The effect of variations in σ at constant crystallinity will be discussed below. In the plots, values of E_s' are normalized by the crystalline modulus E_c' for convenience. Thus we plot E_s'/E_c' versus crystallinity X.

Referring to Figure 2 we see that for the series model (model D) E_s' is not very sensitive to changes in the degree of crystallinity below 90% where E_s'

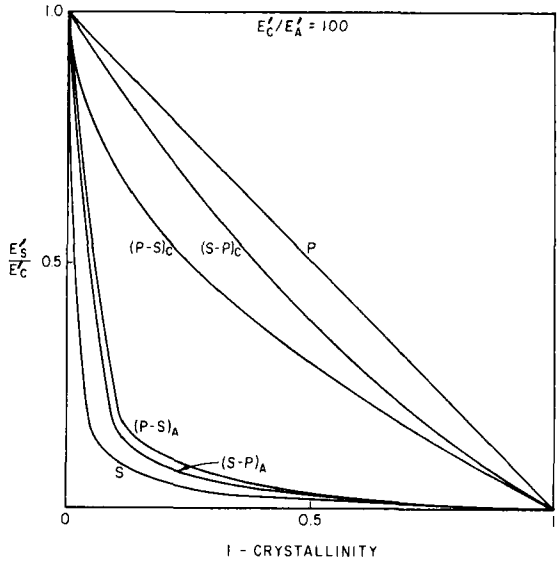

FIGURE 2 Variations in systems modules with crystallinity for various models.

remains very close to E_a'. Almost the entire change in modulus (E_s') occurs in the range of crystallinity between 90 to 100% where dE_s'/dX is positive and very large.

In the parallel model (model A) on the other hand, the relationship between the degree of crystallinity and E_s' is linear.

The responses of the mixed models $(PS)_c$, $(SP)_c$, $(PS)_A$, and $(SP)_A$ to changes in the degree of crystallinity lie between those observed with the series and parallel models.

From the plots of Figure 2, it can be seen that at each level of crystallinity, the maximum in modulus E_s' is obtained with the parallel model and the minimum with the series model. Considering the schematic representation of the six models shown in Figure 1, it is apparent that by adjusting the relative dimensions of the blocks (i.e. by varying σ, the ratio of λ to ϕ) each of the four-mixed models may vary between the simpler series and parallel models. Thus, given a value of the system modulus E_s' and the crystallinity X, it is possible to fit all four models to the data by varying σ. In other words, one value of the system modulus is not sufficient to distinguish between the four models.

The expressions for tan δ_s for the various models as a function of the degree of crystallinity and the geometric parameter σ are given below. (Since these equations are quite complicated, the dependence on crystallinity and σ is included implicitly through λ and ϕ (λ' and ϕ') to simplify the expressions. Tan δ for the crystalline phase is assumed to be zero.)

Model A — parallel

$$\frac{\tan \delta}{\tan \delta_A} = \frac{1}{1 + \left(\frac{\lambda}{1-\lambda}\right) K} \equiv f(\lambda, K) \tag{7}$$

Model B — $(PS)_c$

$$\frac{\tan \delta}{\tan \delta_A} = \frac{\left(\phi, \frac{1}{K}\right)}{1 + \left(\frac{1-\lambda}{\lambda}\right)(1 - \phi + \phi K)} \tag{8}$$

Model C — $(SP)_c$

$$\frac{\tan \delta}{\tan \delta_A} = \frac{f(\lambda, K)}{1 + \left(\frac{1-\phi}{\phi}\right)\left(1 - \lambda + \frac{\lambda}{K}\right)} \tag{9}$$

Model D — series

$$\frac{\tan \delta}{\tan \delta_A} = \frac{1}{1 + \left(\frac{\phi'}{1-\phi'}\right)\frac{1}{K}} \tag{10}$$

Model E — $(PS)_A$

$$\frac{\tan \delta}{\tan \delta_A} = \frac{1 + \left(\frac{\lambda'}{1-\lambda'}\right) f\left(1 - \phi', \frac{1}{K}\right)}{1 + \left(\frac{\lambda'}{1-\lambda'}\right)\frac{1}{1-\phi'+\phi' K}} \tag{11}$$

Model F — $(SP)_A$

$$\frac{\tan \delta}{\tan \delta_A} = \frac{1 + \left(\frac{\phi'}{1-\phi'}\right)\frac{f(1-\lambda', K)}{1-\lambda'+\lambda' K}}{1 + \left(\frac{\phi'}{1-\phi'}\right)\frac{1}{1-\lambda'+\lambda' K}} \tag{12}$$

$$K \equiv \frac{E_c}{E_A'}$$

Plots of the variation of $\tan \delta_s$ with the degree of crystallinity corresponding to these equations are given in Figure 3. As in the plots of E_s', we assume a value of $\sigma = 1$ to allow the demonstration of the general features of the dependence

of tan δ_s on crystallinity. The effect of variations in σ will be discussed below. In the plots, tan δ_s is normalized by tan δ_A (tan δ of the amorphous) so that we plot tan δ_s/tan δ_A versus crystallinity.

From the plots of tan δ_s/tan δ_A shown in Figure 3 it can be seen that for the parallel and crystal matrix models, tan δ_s is very sensitive to changes in

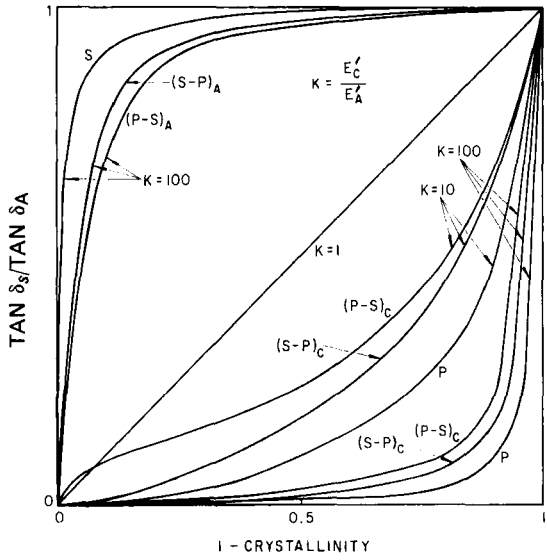

FIGURE 3 Variations in system tan δ with crystallinity for various models.

crystallinity in the range of low crystallinity ($X = 0$ to 0.4). When the degree of crystallinity of the system reaches 50%, tan δ_s is already very small and changes rather insignificantly with further increases in crystallinity.

With the series and amorphous matrix models on the other hand, tan δ_s is very high and relatively insensitive to changes in crystallinity in the range of 0 to 0.6. For values of $X > 0.6$, the ratio of tan δ_s/tan δ_A decreases rapidly reaching the maximum sensitivity (d (tan δ_s/tan δ_A)/$d(1 - X)$ max) at zero degree of crystallinity. As in the case of the system modulus (E_s'), each of the mixed models may be fitted to a simple value of tan δ_s at a particular crystallinity by varying the dimensions of the blocks (i.e. by varying σ). Thus, the determination of one of the independent properties E_s' or tan δ_s is not sufficient to distinguish between the four models, despite the fact that on the average, the properties of models having a crystalline matrix differ considerably from those having an amorphous matrix. This point is illustrated in Figure 4 for systems having 50% crystallinity where we show plots of tan δ_s as a function

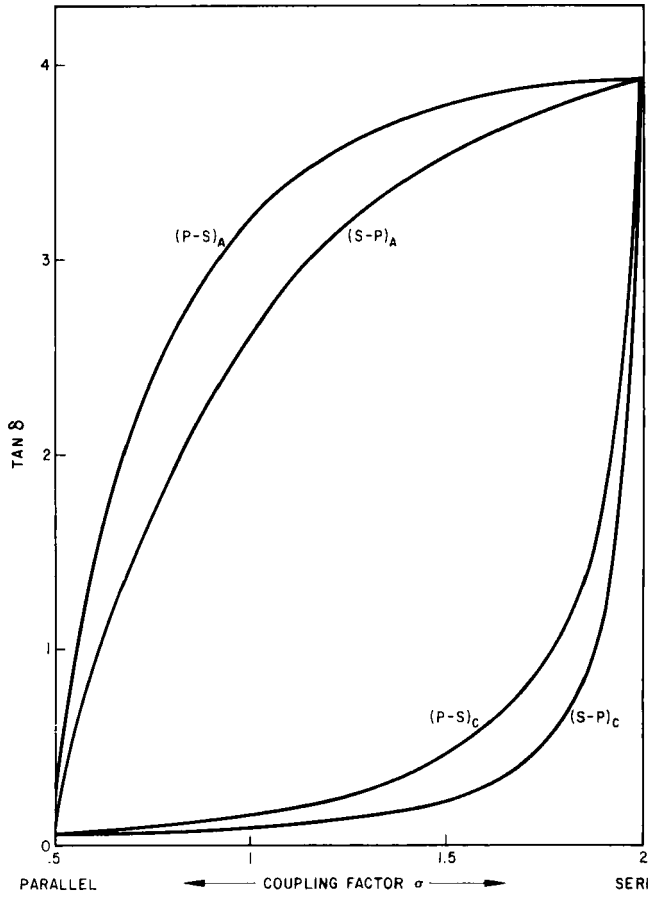

FIGURE 4 Variations in tan δ with σ for crystalline and amorphous matrix models; $X = 50$.

of σ for the crystalline and the amorphous matrix models. From the plots we observe that the amorphous matrix models ($(PS)_A$ and $(SP)_A$) for which $\sigma \geq 0.6$ (which represents $\sim 93\%$ of all possible models) have tan δ_s/tan $\delta_A > 1.0$ while the majority of the crystalline matrix models (those for which $\sigma \leq 1.7$ which represents $\sim 13\%$ of all possible models) have tan δ_s/tan $\delta_A < 1$. Thus, one can use the magnitude of tan δ_s as a guideline for determining which phase (amorphous or crystalline) forms the matrix.

In principle, a definite differentiation between the models having a crystalline matrix $(PS)_c$ and $(SP)_c$ from those having an amorphous matrix $(PS)_A$ and $(SP)_A$ can be made by measuring the two independent properties E_s' and tan δ_s (e.g. on a vibron dynamic viscoelastometer), provided one knows the

corresponding properties of the amorphous and crystalline phases. However, since in many cases it is difficult to obtain these properties (i.e. the crystalline and amorphous complex moduli) a reliable determination of the correct type of model is often precluded.

Effect of Temperature on E_s' and Tan δ_s

A very efficient method for distinguishing between amorphous and crystalline matrix models involves the measurement of changes in E_s' and tan δ_s in a temperature interval involving a transition. This analysis can often be carried out most accurately by examining the behavior of the polymer in a temperature interval involving the glass transition. Frequently, in this temperature range, the effects are very large which is important for achieving good resolution. Furthermore, since the crystalline relaxation usually occurs considerably above the glass transition temperature, it is often possible to study the effects of a single relaxation of one phase on the whole system thus simplifying the analysis.

The principle of the method applied to a single relaxation model conforming to the Arrhenius temperature dependence is outlined below. For a single relaxation model the following expressions are valid:

$$E' = E_R + \frac{(Eu - Er)\omega^2\tau_\gamma^2}{1 + \omega^2\tau_\gamma^2} \tag{13}$$

$$E'' = \frac{(Eu - Er)\omega\tau_\gamma}{1 + \omega^2\tau_\gamma^2} \tag{14}$$

$$\text{Tan } \delta = \frac{(Eu - Er)\omega\tau_\gamma}{Er + Eu\omega^2\tau_\gamma^2} \tag{15}$$

There, Er and Eu are the relaxed and unrelaxed modulus, ω is the frequency and $\tau\gamma$ is the relaxation time.

In order to examine the temperature dependence of the above expressions, we apply the Arrhenius relationship

$$\tau = \tau_O \exp \frac{H}{RT} \tag{16}$$

Here H is the activation energy of the dispersion, τ_O is a constant on the order of magnitude of 10^{-12} sec, T is the absolute temperature and R is the gas constant. By inserting the relationship (16) into Eqs. (13), (14), and (15) we obtain expressions through which the temperature dependence of the dynamic-mechanical properties for such a system may be determined. To

illustrate the typical temperature dependence for an amorphous polymer we may apply these expressions by assuming that the polymer exhibits a maximum in tan δ at 120°C and possesses relaxed and unrelaxed moduli of 10^8 and 10^{10} dynes/cm^2 respectively. (These values are of the right order of magnitude for a major amorphous transition in a semi-crystalline polymer.) Results of these calculations are presented in Figure 5 where we plot E', E'', and

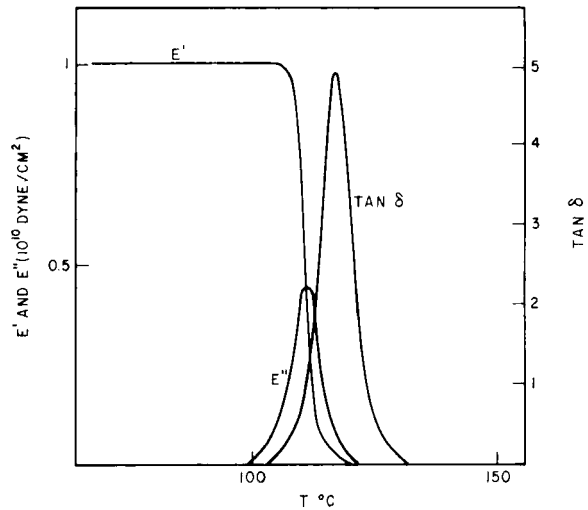

FIGURE 5 E', E'', and tan δ versus temperature for single relaxation Arrhenius model (one phase system).

tan δ versus temperature. From the plots we see that the calculated behavior is quite close to that exhibited by real amorphous polymers, namely, a large tan δ maximum (on the order of 5) and a modulus drop which occurs over a temperature interval of approximately 20 degrees.

By treating this model material as the amorphous phase in a two phase semi-crystalline system, we may examine the effects of load transfer between the phases on the temperature variation of tan δ_s and E_s'. This may be done by inserting the calculated temperature dependence of the amorphous properties (tan δ_A and E_A') into the equations (1 through 12) for the load transfer models presented above. To do this, we assume a crystallinity (X) of 50%, a crystal modulus (E_c) of 100×10^{10} dynes/cm^2, and a low temperature ($T \approx -100$°C) system modulus of 5×10^{10} dynes/cm^2. We then fit each of the models to give the assumed system modulus at −100°C by determining the load transfer factor σ for each. With the models thus completely defined, we insert the temperature dependent amorphous properties (E_A' and tan δ_A) and

calculate the resulting system temperature dependence. From these calculations we obtain the results shown in Figure 6, where we plot tan δ_s and E_s' versus temperature for the various models.

Considering the plot of system modulus (E_s') versus temperature shown in Figure 6, it is apparent that the crystal matrix models ($(PS)_c$ and $(SP)_c$) exhibit a much lower drop in modulus on passing through the amorphous transition than the amorphous matrix models ($(PS)_A$ and $(SP)_A$). The large difference in the response of these classes of load transfer models is also illustrated in the tan δ_s versus temperature plot. Here, the crystal matrix models show a much lower tan δ_s than the amorphous matrix models. Thus, we see that in general the examination of property changes in the glass transition region provides an easy distinction between the amorphous and crystalline matrix models.

The distinction between series-parallel and parallel-series arrangements is, however, much less apparent. The difference between the responses of these

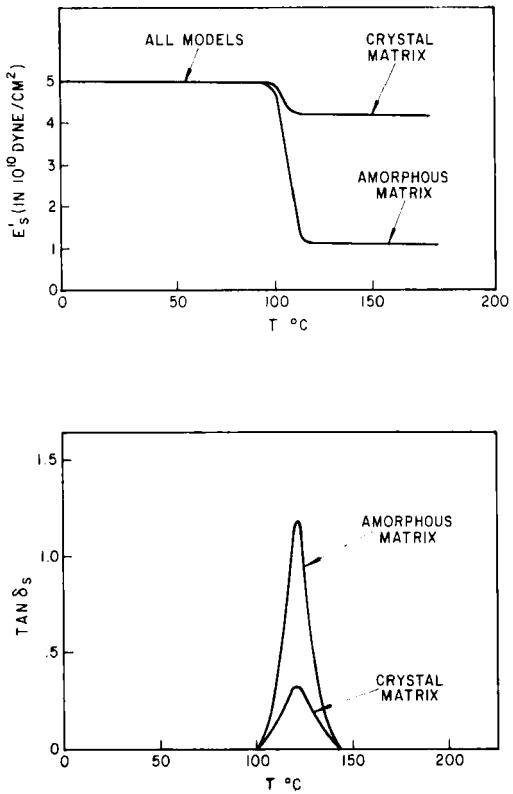

FIGURE 6 E_s' and tan δ_s versus temperature for crystal matrix and amorphous matrix models (two phase system).

models (e.g. between $(PS)_c$ and $(SP)_c$) in both tan δ_s and E_s' is negligible, and thus temperature experiments would prove to be of little use in determining the correct model for a particular system. It must be pointed out however, that the necessity of such a differentiation is questionable since the physical significance of making such a distinction is not understood at this time. Thus, in cases where both the parallel-series and the series-parallel arrangements appear to fit the experimental data, one should proceed by considering solutions for both models.

Coupling Models from Diffusion Studies

The success in determining the appropriate coupling models by means of the previously described methods depends strongly on the accuracy of the estimates of $E_{A,\,u}$, $E_{A,\,R}$, E_c and the relaxation times associated with the transition. For many polymers this information is not readily available. In the absence of such information it is possible to establish the nature of coupling from a series of diffusion experiments carried out above the glass transition temperature. This approach is based on the following considerations.

It has been shown that Eq. (17) holds for diffusion in amorphous polymers in the rubbery state

$$ln \frac{D}{RT} = - B ln\tau + C \tag{17}$$

Where D_T is the diffusion coefficient, R is the gas constant, B and C are constants depending on the chemical structure of the polymer and penetrant, and T is the absolute temperature.

It has also been shown that

$$B = \frac{\Delta H_v}{\Delta H_B} \tag{18}$$

where ΔH_v and ΔH_B are respectively activation energies of viscous flow and diffusion. In cases where the size of the diffusing molecule is comparable to the size of the polymer segment that moves, $H_v = H_B$ and $B = 1$. This has indeed been observed.

Consider now a diffusion process in a semi-crystalline polymer above the glass transition temperature, where the crystalline phase is essentially impermeable for the diffusing molecules. For the "microdiffusion" within an amorphous domain, (17) is still applicable and can be written:

$$ln \frac{D_a}{RT} = - B_a ln\tau_a + C_a \tag{19}$$

where subscript "a" denotes that the particular quantities refer to the amorphous phase only. In order to obtain an analogus expression valid for the

diffusion processes in the more complicated two phase system of semi-crystalline polymers, one may apply the empirical Eq. (20):

$$D = \phi_a{}^m D_a \tag{20}$$

where ϕ_a is the degree of amorphicity and "m" is a factor depending on the tortuosity of the permeable channels. It should be noted that if the geometrical features of the permeable and impermeable phase are known, "m" can be computed with reasonable accuracy. Results of such calculations in the literature correlate well with experimental determinations of "m" and show that "m" falls in the range between 0.3 and unity.

Rewriting (20) in logarithmic form and accounting for the temperature effects:

$$ln \frac{D}{RT} = mln\phi_a + ln \frac{D_a}{RT} \tag{21}$$

and combining (21) with (19) we obtain

$$ln \frac{D}{RT} = -B_a ln\eta_a + C_a + mln\phi_a \tag{22}$$

Considering that η_a cannot be measured, it is desirable to define a relationship between the sample viscosity (η) which can be measured, and the amorphous viscosity (η_a). For this purpose we make use of

$$\eta = \phi_a{}^n \eta_a \tag{23}$$

where "n" is a constant related to the load transfer between the phases. It follows from (22) and (23) that

$$ln \frac{D}{RT} = -B_a (-nln\phi_a + ln\eta) + C_a + mln\phi_a \tag{24}$$

which leads to:

$$ln \frac{D}{RT} = -B_a ln\eta + C_a + B_a ln\phi_a{}^n + ln\phi_a{}^m \tag{25}$$

and:

$$ln \frac{D}{RT} = -B_a ln\eta + C_a + ln (\phi_a{}^{m+nB_a}) \tag{26}$$

An inspection of (26) indicates the complex relationship between the structure of the amorphous phase (B_a, C_a), degree of amorphicity (ϕ_a), size and arrangement of crystallites (m), load distribution between phases (n) and viscosity of the sample (η).

In applying Eq. (26) for the interpretation of the diffusion results in terms of polymer structure (degree of crystallinity, size of crystallites, orientation of the amorphous phase, etc.) or for the determination of the load transfer coefficient "n" it should be noted that:

1) Sample viscosity can be estimated from dynamic experiments by means of E''/ω where ω = the frequency of the experiment.
2) C_a, B_a, ϕ_a, m and n are constants independent of temperature.
3) With samples of the same amorphous orientation, B_a is independent of ϕ_a.

RESULTS AND DISCUSSION

Coupling Models for Undrawn Nylon-6

A series of unoriented Nylon-6 samples of various degree of x-ray crystallinities was examined with respect to E', E'', and tan δ in the temperature range between $-80°$ to $+150°$C. The measurements were carried out at a frequency of 110 cycles/sec by means of the Vibron type viscoelastometer. The pertinent x-ray data and the values of (tan δ) max of the α relaxation are given in Table I.

Since it is difficult to prepare specimens of Nylon-6 of very low crystallinity and since such specimens cannot be examined over a wide temperature range without changing the crystallinity, we include in the analysis which follows a series of cross-linked Nylon-6 samples. These polymers were prepared with small amounts of hexamethylene diamine and trimesic acids using the following procedure:

Forty grams of mixtures of freshly distilled dry (50 p.p.m. water) ϵ-caprolactam (CL) and various amounts of both hexamethylene diamine (HMDA) and trimesic acid (TMA) were heated to 160°C under a stream of dry helium. Subsequently, the tubes were sealed off (under helium) and allowed to

TABLE I
Degree of Crystallinity and (Tan δ) max for unoriented Nylon-6 Polymers

Specimen	Degree of Crystallinity (%)	(Tan δ) max
1	35	0.15
2	42	0.14
3	45	0.12
4	50	0.10
5	55	0.08

polymerize at 260°C for 48½ hours. The products were then milled, water extracted, vacuum dried, and compression molded into films of 5 mils thickness for x-ray analysis and determination of viscoelastic properties. The pertinent data relating to these films are presented in Table II.

TABLE II
Characteristics of Experimental Cross-linked Poly-caprolactams

Sample	Initial Composition % by weight CL/TMA/HMDA	X-ray Analysis % amorphous	% α	% β	(tan δ) max α' relaxation
1	97.5/1.0/1.5	47	17	36	0.18
2	92.5/3.0/4.5	47	16	37	0.22
3	90.0/4.0/6.0	68	8	24	0.38
4	87.5/5.0/7.5	~100	0	0	0.78
5	85.0/6.0/9.0	~100	0	0	0.92
6	100/ 0/ 0	45	50	5	0.13

The variation of tan δ max (α' transition) with the degree of crystallinity for the Nylon-6 films and the cross-linked polycaprolactams are plotted in Figure 7. From these plots we observe that the general form of the variation of tan δ max with crystallinity closely resembles that of systems in which the crystalline phase forms the load-transfer matrix (see Figure 3). Thus, we assume that for undrawn Nylon-6 the crystal matrix models apply. We also observe from Figure 7 that the value of tan δ max approaches a value of about one as the crystallinity approaches 0%, and thus, we assume that tan δ max for the amorphous phase is close to unity. With these observations, we proceed to determine the value of the load transfer parameter σ for the parallel-series crystal matrix model which applies to undrawn Nylon-6 at 50% crystallinity. That is, we fit the coupling model to the experimental data obtained.

For this purpose, we write the general equation relating the complex modulus of the system (E_s^*) to the properties of the separate phases for the parallel-series crystalline matrix model in which the crystalline phase shows no relaxation:

$$\frac{E_s^*}{E_c} = \lambda\left(\frac{\phi\alpha + (1-\phi)(\alpha^2+\beta^2) + i\phi\beta}{(1-\phi)^2(\alpha^2+\beta^2) + \phi^2 + 2\phi(1-\phi)\alpha}\right) + (1-\alpha) \qquad (27)$$

in this relation,

$E_c \equiv$ modulus of the crystalline phase

$$\alpha \equiv \frac{E_A'}{E_c}$$

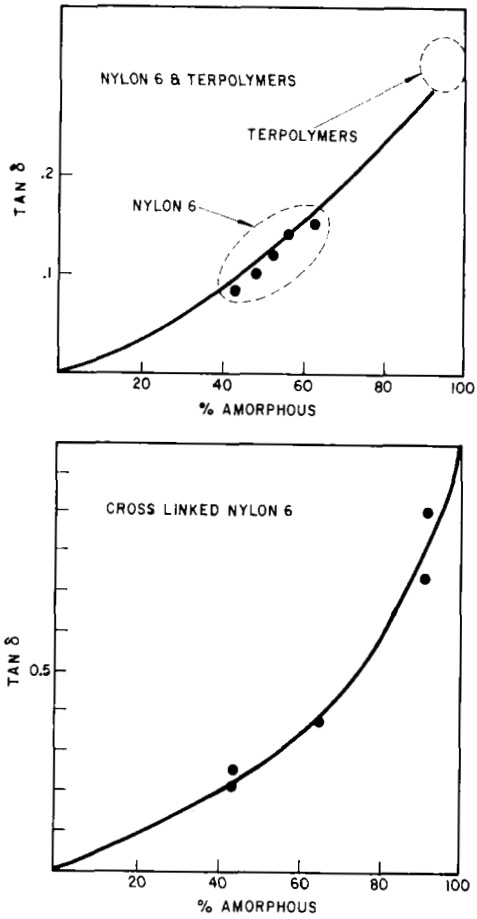

FIGURE 7 Intensity of α' peak in tan δ versus amorphous content for various Nylon-6 polymers.

$$\beta \equiv \frac{E_A''}{E_c}$$

$\lambda \equiv$ vertical dimension of the amorphous block

$\phi \equiv$ horizontal dimension of the amorphous block

We now apply this equation to temperatures below and above the amorphous relaxation. Here $\beta = 0$ and $\alpha \ll 1$. Thus, the equation reduces to

$$\frac{E_s^*}{E_c} = \frac{E_s'}{E_c} \approx \frac{\lambda}{\phi}\alpha + (1 - \lambda)$$

Rewriting this by considering the definitions of the various parameters, we get

$$\frac{E_s'}{E_c} \approx \sigma \frac{E_A'}{E_c} + (1 - \lambda)$$

or

$$\frac{E_A'}{E_c} \approx \frac{1}{\sigma}\left(\frac{E_s'}{E_c} - (1 - \lambda)\right) \tag{28}$$

By applying this relationship below and above the amorphous relaxation, we obtain

$$\frac{E_A'{}_L}{E_c} \approx \frac{1}{\sigma}\left(\frac{E_s'{}_L}{E_c} - (1 - \lambda)\right)$$

and

$$\frac{E_A'{}_H}{E_c} \approx \frac{1}{\sigma}\left(\frac{E_s'{}_H}{E_c} - (1 - \lambda)\right)$$

where the subscripts "L" and "H" imply low and high temperature respectively. Taking the ratio of these equations we obtain

$$\frac{E_A'{}_H}{E_A'{}_L} = \frac{E_s'{}_H - (1 - \lambda)\, E_c}{E_s'{}_L - (1 - \lambda)\, E_c} \tag{29}$$

Now, since we measure $E_{s\ L}$ and $E_{s\ H}$ and since $E_{A\ H}/E_{A\ L}$ is related to tan δ_A max (which we know) via

$$\tan \delta_A \text{ max} = \frac{1 - (E_A'{}_H/E_A'{}_L)}{2\,(E_A'{}_H/E_A'{}_L)^{1/2}}$$

(This equation is obtained from Eq. 19 by observing that tan δ is maximum at $\omega\tau\gamma = (E_A'{}_H/E_A'{}_L)^{1/2}$). We have thus determined a relationship between λ and the crystal modulus E_c such that the experimental data $(E_s'{}_L/E_s'{}_H)$ is satisfied. To cast the relationship in more concrete terms, we apply the experimentally determined values:

$$E_s'{}_L = 2.0 \times 10^{10} \text{ dynes/cm}^2 \quad (0°\text{C})$$

$$E_s'{}_H = 0.65 \times 10^{10} \text{ dynes/cm}^2 \quad (150°\text{C})$$

$$\tan \delta_A \text{ max} = 1 \Rightarrow \frac{E_A'{}_H}{E_A'{}_L} \approx 0.17$$

to obtain

$$\lambda = 1 - \frac{0.37 \times 10^{10}}{E_c}$$

Now, since $\lambda = \sqrt{\sigma (1 - X)}$ and $X = 0.5$ (50% crystallinity)

we obtain $\sigma = 2\left(1 - \dfrac{0.37 \times 10^{10}}{E_c}\right)^2$ (30)

Thus, given a value of the crystalline modulus, we can determine the coupling parameter. However, reliable values of crystalline moduli are not available since their measurement requires an *a priori* assumption regarding the load transfer between the phases. Hence, we must obtain additional information if the problem is to be solved.

For this purpose, we recall Eq. 27

$$\frac{E_s^*}{E_c} = \lambda \left(\frac{\phi\, a + (1 - \phi)(a^2 + \beta^2) + i\phi\beta}{(1 - \phi)^2 (a^2 + \beta^2) + \phi^2 + 2\phi (1 - \phi)\, a} \right) + (1 - a) \tag{28}$$

Applying the approximation used above, we obtain an expression for the system loss (imaginary) modulus (E_s'')

$$\frac{E_s''}{E_c} \approx \phi\beta = \phi \frac{E_A''}{E_c}$$

or

$$\frac{E_s''}{E_A''} \approx \phi \tag{32}$$

Now E_A'' is related to $E_A'_H$ and $E_A'_L$ by Eq. 18.

$$E_A'' = \frac{(E_A'_L - E_A'_H)\, \omega\tau_\gamma}{1 + \omega^2 \tau_\gamma^2} \tag{33}$$

If we now apply this equation at the temperature at which tan δ is maximum, we obtain

$$E_A'' = \frac{(E_A'_L - E_A'_H)(E_A'_H/E_A'_L)^{1/2}}{1 + (E_A'_H/E_A'_L)}$$

Inserting the value of $E_A'_H/E_A'_L = 0.17$
this reduces to

$$E_A'' = 0.29\, (E_A'_L)$$

On inserting this relation and the value of E_s'' into Eq. (32) we obtain

$$\sigma = 0.41 \times 10^{10}/E_A'_L$$

Thus, we have obtained a relationship between the coupling parameter σ and the low temperature (i.e. unrelaxed) amorphous modulus which must be satisfied to be consistent with the experimental data. Recalling the relationship determined above on the basis of system modulus data

$$\sigma = 2\left(1 - \frac{0.37 \times 10^{10}}{E_c}\right)^2$$

we see that we now have two equations in the three unknowns σ, $E_A'_L$, and E_c. This relationship is presented in Figure 8 where we plot E_c and $E_A'_L$ versus σ. Thus, for example, given the value of E_c we can determine the coupling parameter σ and the low temperature amorphous modulus ($E_A'_L$).

To obtain an estimate of E_c we observe that the effective value of E_c for an unoriented system is approximately given by the average of the modulus in the direction of the polymer chains in the crystal ($E_{//}$) and that perpendicular to it ($E_\perp$).

For an estimate of the value of $E_{//}$ we consider Treloar's[3] calculated crystal modulus of $E_{//} \approx 200 \times 10^{10}$ dynes/cm^2. Since the Treloar calculations assume a fully extended chain in the crystal, this value obviously represents the upper bound on $E_{//}$. The experimental values of Sakurada[4] ($E_{//} \approx 20 \times 10^{10}$ dynes/cm^2) for Nylon-6 on the other hand, are based on the assumption of a series model in an oriented system which, as we shall see below, is incorrect and for reasons stated in the introduction we must regard this value as a lower bound on $E_{//}$. Using the results of our load transfer

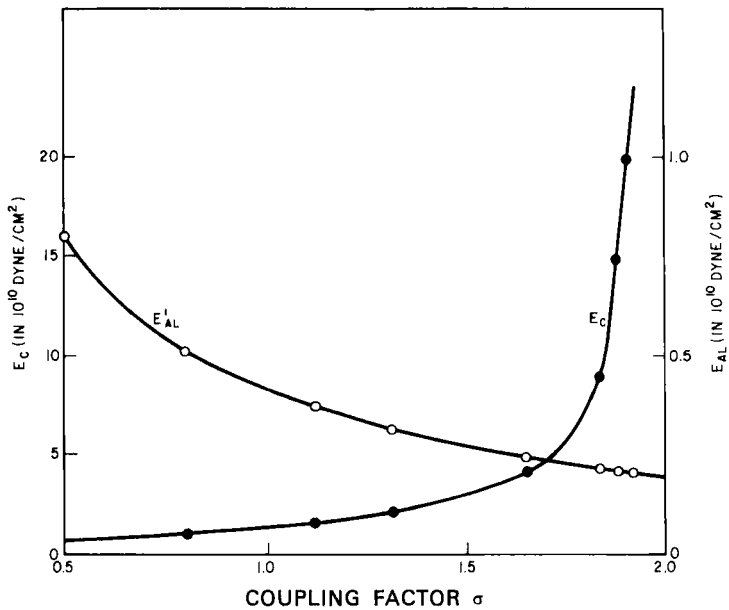

FIGURE 8 Unoriented Nylon-6: Plots of crystalline and amorphous modulus versus coupling factor σ; values satisfying the experimental data.

studies on oriented Nylon-6 we estimate the error of Sakurada to be on the order of 20%. Thus, we imply that $E_{//} \approx 25 \times 10^{10}$ dynes/cm^2.

The value of the average transverse modulus ($E_{\perp}$) is assumed, on the basis of experimental data, to be on the order of 4×10^{10} dynes/cm^2. Thus, the effective crystal modulus in unoriented systems (E_c) is approximately 15×10^{10} dynes/cm^2. Using this value and the data of Figure 8, we arrive at the following values for the coupling parameter σ and low temperature (unrelaxed) amorphous modulus of

$$\sigma \cong 1.88$$

$$E_A'{}_L \cong 0.22 \times 10^{10} \text{ dynes/cm}^2$$

Thus, for undrawn Nylon-6 film of 50% crystallinity we conclude that the following coupling model is valid:

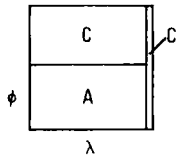

$$\lambda/\phi = 1.88$$

this indicates a very inefficient structure with respect to the potential reinforcement of the system by the crystalline phase.

Coupling Model of Oriented Nylon-6 Fibers from Diffusion Studies

The diffusion Eq. (26) was applied to a series of experimental Nylon-6 fibers. These were examined with respect to the degree of amorphous fraction, coefficient of diffusion, sample viscosity, size of crystallites and degree of orientation of the amorphous phase. This latter information was estimated by means of the expression derived by Stein[5]

$$\Delta = X f_c \Delta_c^\circ + (1 - X) f_a \Delta_a^\circ \tag{31}$$

Here Δ is the measured birefringence, X is the degree of crystallinity, f_c and f_a are the crystalline and amorphous orientation functions, and Δ_c° and Δ_a° are the birefringences of a segment in the crystalline and amorphous phases. For Nylon-6

$$\Delta_c^\circ = \Delta_a^\circ = 0.073$$

Values of f_c, defined as $f_c = 1/3\ (3\ \overline{\cos^2 \phi} - 1)$ were estimated by the method of Dumbleton using the azimuthal width of the 200 reflections. The pertinent data of these studies are summarized in Tables III and IV.

TABLE III

Amorphous and Crystalline Orientation Functions of Experimental Nylon-6 Yarns

	III	IV	V
Half Angle (200) & (202 + 002)	9°	10°	13°
Birefringence, Δ	.0469	.0515	.0528
Degree of Crystallinity, X	.42	.49	.57
Crystalline orientation function, f_c	.933	.925	.888
Amorphous orientation function, f_{am}	.409	.495	.503

TABLE IV

Sample viscosity, coefficient of diffusion and degree of amorphicity of experimental Nylon-6 fibers

Sample Symbol	$\left(\frac{C_1}{C\infty}\right)^2 \sim D$	$\eta = E''/\omega$	ϕ_a
I	.144	.90 × 10^6poise	.32
II	.140	.99 ,,	.58
III	.085	.94 ,,	.51
IV	.073	1.07 ,,	.46
V	.107	.92 ,,	.43

where C_1 = dye uptake in 10 minutes
$C\infty$ = dye uptake at equilibrium
D = diffusion constant, proportional to $\left(\frac{C_1}{C\infty}\right)^2$
E'' = loss modulus measured at 35°C, 95% R.H., 110 cps
ω = 2π (frequency) = 2π (110)
ϕ_a = amorphous volume fraction

Here it can be seen that in samples I, III, and V we have a series of fibers of nearly equal viscosity (0.90, 0.94, and 0.92 × 10^6 poise respectively) and different amorphicity, (0.32, 0.51, and 0.43 respectively). Considering further that at least samples I and III have nearly equal total and amorphous orientation and consequently nearly equal B_a, we can plot for these samples $ln\ D$vs. $ln\phi_a$ to obtain the value of the exponent $(m + nB_a)$. The corresponding plot shown in Figure 9 indicates a slope of −1.12. Consequently, we assume that for this series

$$m + nB_a = -1.12. \tag{35}$$

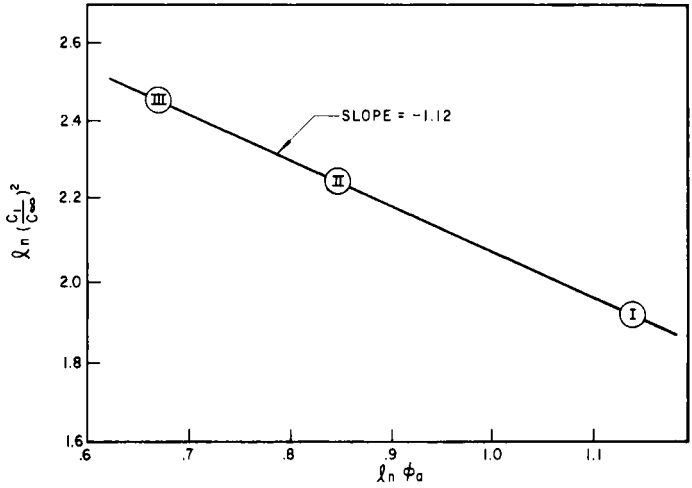

FIGURE 9 Logarithmic plot of diffusion coefficient versus degree of amorphicity; sample viscosity (E''/ω) and amorphous orientation (i.e. B_a) are constant.

Again referring to the data in Table IV we see that samples IV and V have nearly the same amorphous content (.46 and .43 respectively). Assuming that C_a does not vary greatly between these samples we extract a value for B_a by calculating $\Delta lnD/\Delta ln\eta$. The result is $B_a = 2.4$.

Based on the x-ray data concerning the size of the crystallites we inferred that within this series "m" should be considered constant at least as far as the dimensions of the crystallites perpendicular to the fiber axis are concerned. The maximum difference in crystallite size within the series is about 13% which is far too small to affect significantly the length of the path of the diffusing molecules from sample to sample. From geometrical considerations we then concluded that the path of penetrating molecules is approximately 1.5 times as long as it would be without the crystallites. This assumption leads to a value of $m = 0.5$.

Following these considerations, we insert the values for B_a and m into Eq. (35) yielding

$$0.5 + n(2.4) = -1.12$$

or

$$n = -0.68$$

Returning to the basic Eq. (26) and inserting the values of parameters (B_a, n, m) we obtain

$$ln\left(\frac{D}{RT}\right) = -2.4\, ln(E''/\omega) + C_a + ln\phi_a^{-1.12} \tag{36}$$

Eq. (36) is then used to plot calculated and measured coefficients of diffusion shown in Figure 10. Assuming a value of C_a of 1.38×10^{13} we were able to obtain a nearly perfect fit of the results from fibers having nearly equal amorphous orientation. This behavior was expected because of the known sensitivity of B_a to amorphous orientation. Thus establishing the validity of (26) we proceed with the analysis of the coupling model from the extracted value of "n".

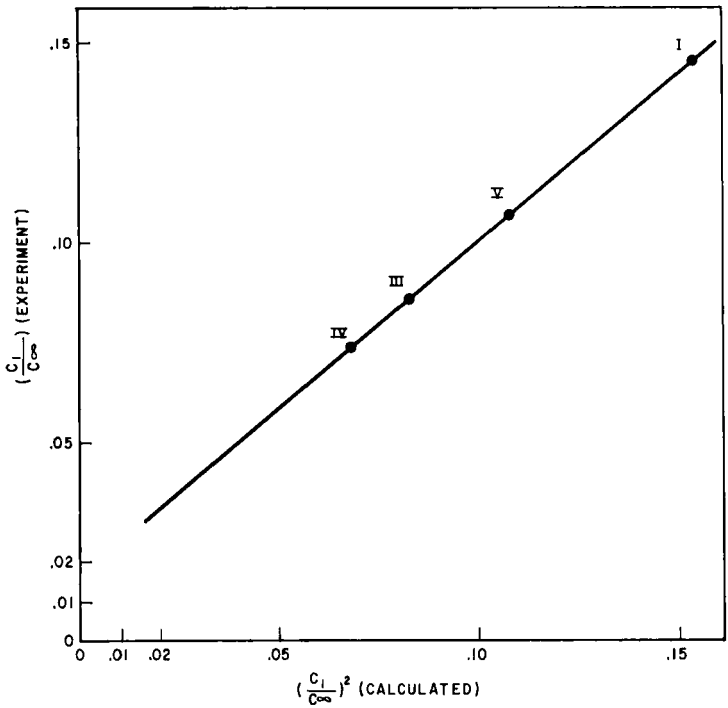

FIGURE 10 Calculated and measured coefficient of diffusion for experimental Nylon-6 fibers.

From the magnitude of the tan δ peak of the a' transition for these fibers (tan $\delta \approx 0.11$) and the plots of Figure 3, one can infer that these fibers conform to a crystalline matrix model (either $(SP)_c$ or $(PS)_c$). From considerations of the anisotropy of modulus and tan δ observed in drawn Nylon-6 systems, we can also infer that the $(PS)_s$ model is the more probable. For this model we have

$$\frac{E_s''}{E_A''} \approx \frac{\phi_a}{\left(\phi\left(1-\frac{1}{K}\right)+\frac{1}{K}\right)^2} \tag{37}$$

where ϕ is the vertical dimension of the amorphous block, ϕ_a is the degree of amorphicity, and $K \equiv E_c'/E_A'$.
In cases where $K \gg 1$, this equation reduces to

$$E_s''/E_A'' \approx \frac{\phi_a}{\phi^2} = \frac{\lambda\phi}{\phi^2} = \frac{\lambda}{\phi} = \sigma \tag{38}$$

Such conditions obtain (i.e. $E_c'/E_A' \gg 1$) for temperatures above the a' relaxation, where we have also shown that

$$E_s'' \approx E_A''\,\phi_a^{-0.68} \text{ for } 0.3 < \phi_a < 0.6 \tag{39}$$

Thus, combining the equations (38) and (39) we obtain an expression for the load transfer parameter σ as a function of the amorphous fraction ϕ_a:

$$\frac{E_s''}{E_A} \approx \phi_a^{-0.68} \approx \sigma \quad \text{which is valid for } 0.3 < \phi_a < 0.6$$

Thus, for this series of fibers we conclude that

$$\sigma \approx \frac{1}{\phi_a^{0.68}} \quad \text{for } 0.3 < \phi_a < 0.6$$

To illustrate this variation of the load transfer parameter σ with varying degrees of amorphicity we present schematic representations of the model below.

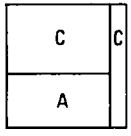

$\phi_a = 0.35$
$\sigma = 2$

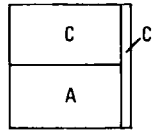

$\phi_a = 0.45$
$\sigma = 1.7$

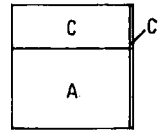

$\phi_a = 0.55$
$\sigma = 1.5$

SUMMARY AND CONCLUSION

A new method is outlined to study the structure property relationship in semicrystalline polymers. The proposed method involves: a) the characterization of structure in terms of the two phase amorphous-crystalline model

(size, concentration, and orientation of the crystallites, etc.) b) the analysis of mechanical coupling between phases in terms of Takayanagi[1] models, and c) the interpretation of mechanical properties assuming a two phase composite system. It is expected that such a study will lead to a better understanding of the nature of the phase boundary and thus provide the information which is essential for the interpretation of the mechanical responses in terms of morphological characteristics (degree of crystallinity, sizes of crystallites, orientation, etc.).

The principles are reviewed for quantitative determination of the load transfer characteristics between the amorphous and crystalline phase in terms of Takayanagi models. A theory is developed to account for the temperature dependence of various system models in a temperature interval involving a transition of the low modulus (amorphous) phase. The derived equations are applied to elucidate the load transfer characteristics of unoriented Nylon-6. It is shown that 1) the a' transition of this polymer involves a relaxation mechanism which can be described well by a single relaxation process conforming to the Arrhenius temperature relation and 2) the unoriented structure is very inefficient with regard to crystal reinforcement. Since the success of the analysis of the temperature effects depends on the availability and accuracy of the unrelaxed and relaxed moduli (E_U and E_R) of the amorphous phase as well as on the relaxation spectrum associated with the transition, the applicability of the method is rather limited.

An alternate approach to determine the coupling models is developed based on the relationship between diffusion and viscoelastic characteristics of the polymer. This approach, which does not require an accurate estimate of the properties of a "completely" amorphous polymer, is applied to a series of oriented Nylon-6 fibers. The study, which confirms the validity of the derived equation to describe the diffusion process in semicrystalline polymers above the glass transition temperature, leads to a quantitative representation of the "efficiency" of crystal reinforcement as a function of the degree of crystallinity.

In connection with the application of diffusion to study the nature of the mechanical coupling between phases it must be pointed out that:

a) the diffusion of small molecules is one of the most powerful methods to investigate the polymer structure.†

b) the diffusion process cannot be interpreted in terms of the results obtained by means of standard characterization techniques.

†Specifically, the diffusion studies led to the concepts of
1) Various degrees of order (in contrast with a two phase system implied from x-ray diffraction).
2) Fluctuations in density of the amorphous phase.
3) Existence of holes in the amorphous phase.
4) Distribution of hole dimensions.

c) the diffusion studies provided the information regarding the structure of the amorphous phase and distribution of crystallites which complements the data provided by standard characterization techniques.

Based on these considerations it is possible that the most important results of the study presented lies in the development of a theory which makes possible the investigation of effects of morphology of semicrystalline polymers on their mechanical properties by means of an analysis involving the results of diffusion, viscoelastic responses, and standard morphological characterization techniques.

References

1. Y. Takayanagi, *Rept. Progr. Polymer Phys.* (Japan), **6**, 121 (1963).
   Y. Takayanagi, *Mem. Fac. Eng. Kyushi Univ.*, 23, No. 1, p.1. (1963).
2. H. Fujita, A. Kishimoto, and K. Matsumoto, *Trans. Faraday Soc.* **56**, 424 (1960).
3. L. R. G. Treloar, *Polymer* **1**, 95 (1960).
4. I. Sukurada, I. Taisuke, and K. Nakamae, *J. Polymer Sci.* Part C, No. 15, 75 (1966).
5. R. S. Stein and F. H. Norris, *J. Polym. Sci.* **21**, 381 (1956).